inter.noise
HAMBURG 2016

Influence of Tire Deformation on Sound Pressure Level inside a Tire

Yohsuke TANAKA, Shogo HORIKAWA and Shigeru MURATA

Kyoto Institute of Technology, Japan

ABSTRACT

In this study, we investigated the influence of the tire deformation on sound pressure level inside a tire around the first cavity resonance frequency in the range from 180 to 280 Hz. The tire was deformed by changing the value of tire pressure in the range from 100 to 300 kPa at a constant load of 400 kN. The distribution of sound pressure level inside a tire was measured by using a test bench with the multi-microphone system. We will show the relationship between the difference between horizontal and vertical mode frequencies and the sound pressure level averaged inside a tire.

Keywords: First tire cavity resonance, Horizontal mode, Vertical mode, Tire pressure, Sound pressure level
I-INCE Classification of Subjects Number(s): 11.7

1. INTRODUCTION

Car manufacturers have been developing electric vehicles (EVs), which include plug-in hybrid EVs (PHEVs), battery EVs (BEVs), and fuel cell EVs (FCEVs) for demand of efficient vehicles caused by fluctuating oil prices. Moreover, EVs will be important to countries for CO_2 reduction in the long term. In these vehicles, tire noise is now more noticeable because noise sources such as an engine-exhaust noise has been reduced.

The tire noise is divided into exterior and interior noises. Exterior noises are radiated from air pushed between the tread patterns and the road surface (1, 2). Interior noises are transferred from the road and tires, wheels and spindles to car interior radiation (3, 4, and 5). Especially, tire cavity resonance is an important interior noise in the range of 200-300 Hz. Noticeable two peaks have horizontal and vertical modes, respectively (3, 5, 7). Therefore, these modes vibrating vehicle spindles in the vertical and horizontal directions results in structure-borne noise.

It is shown theoretically and experimentally that these frequencies depend on the geometrical parameters of a deformed tire (3, 6, and 7). In contrast, there is no theoretical analysis on the pressure distribution inside the tire, except for the pressure distribution in the undeformed tire (8), but there is numerical analysis (9). However, it is not clear the influence of the parameters on pressure distributions inside the tire around these frequencies.

In this paper, we investigated the influence of the tire deformation on sound pressure level inside a tire around first cavity resonance frequency in the range of 180 to 280 Hz by using the developed multi-microphone system (10). A tire was deformed by a constant load of 4 kN with tire pressures in the range of 100 to 300 kPa.

2. DEFORMED TIRE

The sound inside an undeformed tire is treated as a plane wave at lower frequencies in the case of the wavelength which is much greater than the circumferential length, L_c, of a tire. The natural frequency, f_n, of the first tire cavity resonance is derived as

$$f_n = \frac{c}{L_c} \tag{1}$$

where c is the speed of sound in air. The loaded tire cavity has a region of smaller cross section in the area where the tire contacts the road surface with the length of the contact patch, L_{cp}, as shown in Fig. 2.

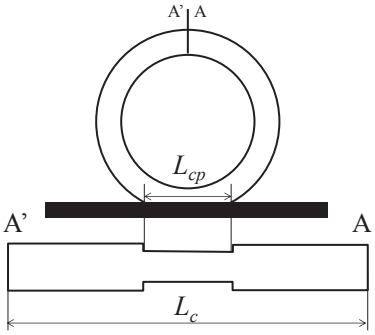

Figure 1 Acoustic model of a deformed tire

The deformed tire produces horizontal and vertical modes around the first resonance (3). Two resonance frequencies are identified as f_1 and f_2, respectively (6).

$$f_1 = \frac{c}{L_c + (1-m)L_{cp}} \tag{2}$$

$$f_2 = \frac{c}{L_c - (1-m)L_{cp}} \tag{3}$$

where m is the ratio of the undeformed cross-sectional area to the deformed cross-sectional area in the contact patch. Comparing these frequencies obtained by Eqs. (1), (2) and (3), they have the relationship $f_1 < f_n < f_2$. The difference between the two frequencies is derived as follows.

$$\Delta f = f_2 - f_1 = \frac{2c(1-m)L_{cp}}{{L_c}^2 - (1-m)^2{L_{cp}}^2} \tag{4}$$

3. EXPERIMENT SETUP FOR MEASURING SPL DISTRIBUTION INSIDE A DEFORMED TIRE

The sound pressure level distributions inside a tire was measured by using a multi-microphone system (MMS) (10) shown in Fig. 2. The tire size was 195/65R15 91S and the diameter is 634 mm; the tire pressure, P_t, was in the range of 100 to 300 kPa. A signal generator (FGA5050GC, Kikusui Electronics) was used to automatically generate a sine wave (pure tone) sound in the range from 180 to 280 Hz, and the speaker vibrates the tire as an acoustic vibrator. A hydraulic jack shown in Fig. 2 (a) deformed the tire with a load of 4 kN as the weight of a sedan. Microphone sensors of MMS were installed in the circumferential direction at 45 degree intervals to resolve the first mode as shown in Fig. 2 (b). The microphone (WM-61A, Panasonic) was attached to an air-proof sensor head.

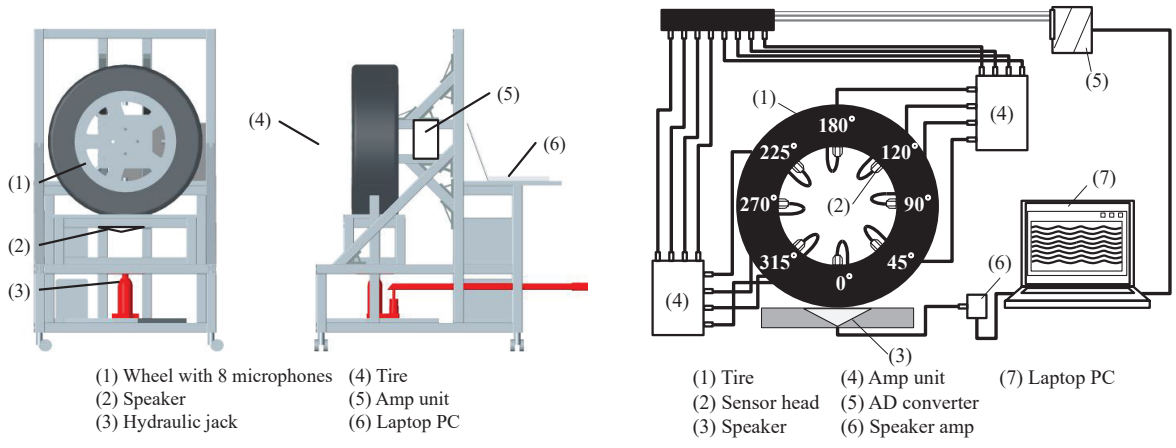

(a) Test bench (b) Multi-microphone system

Figure 2 Experimental setup for measuring SPL distributions inside tire

L_{cp} in Eqs. (2) and (3) was obtained as the width of a tire-print as shown in Fig. 3 (a). Figure 3 (b) illustrates that the L_{cp} becomes larger with decreasing tire pressure. The ratio, m, of the undeformed cross-sectional area to the deformed cross-sectional area was measured by using a contour gauge as shown in Fig. 4 (a). Figure 4 (b) indicates the ratio shows the tendency to increase with tire pressure. L_c is determined by the c/f_n, where f_n was obtained by the cavity resonance frequency of the undeformed tire. In this experiment, the resonance frequency and the speed of sound were f_n = 229 Hz and c = 343.5 m/sec, respectively.

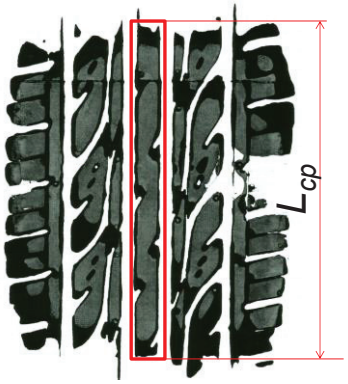

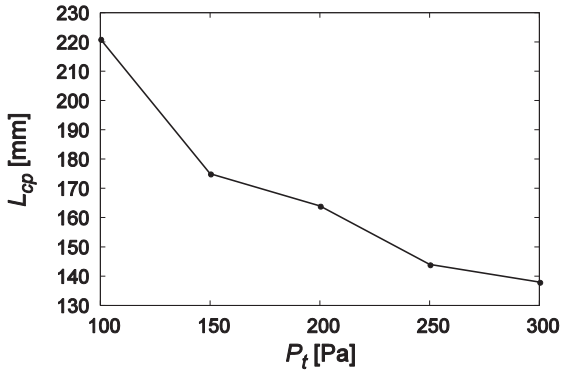

(a) Measurement of length of contact patch (b) Length, L_{cp}, with respect to tire pressure

Figure 3 Length of contact patch, L_{cp}, and tire pressure P_t

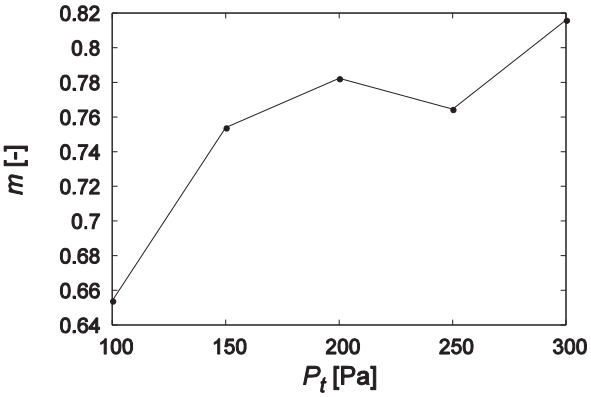

(a) Measurement of cross-sectional area (b) Ratio m with respect to tire pressure

Figure 4 Ratio, m, of undeformed cross-sectional area to deformed cross-sectional area and tire pressure P_t

4. RESULTS

Figures 5 (a) and (b) show the sound pressure level distributions inside a tire are plotted at f_1 and f_2, at each tire pressure. These modes have horizontal and vertical mode shapes. The SPL value of vertical mode remains stable at each pressure. On the other hand, that of horizontal mode decreases with high pressure. Channel average SPL, SPL_{ch}, is averaged by SPL values detected with eight microphone sensors inside a tire. The values of the SPL are plotted with respect to frequency at each tire pressure in Fig. 5 (c). It seems that two peaks are gradually merging into one peak. Figure 6 (a) illustrates differences, Δf_{exp}, between horizontal and vertical mode frequencies become smaller as tire pressure is higher. The differences are appropriate values which are basically in agreement with theoretical values, Δf_{th}, obtained by Eq. (4) as plotted in Fig. 6 (b). Frequency average SPL, SPL_f, averaged by SPL_{ch} in the range of 180 to 280 Hz is plotted with respected with the difference, Δf_{exp}, in Fig. 7. This graph illustrates the SPL increases with the difference. If the difference is large, the SPL increases over a wide frequency range due to occurrence of the sides of two peaks. In order to suppress the SPL around the first tire cavity resonance, parameters of Eq. (4) must be chosen such that the difference is minimized.

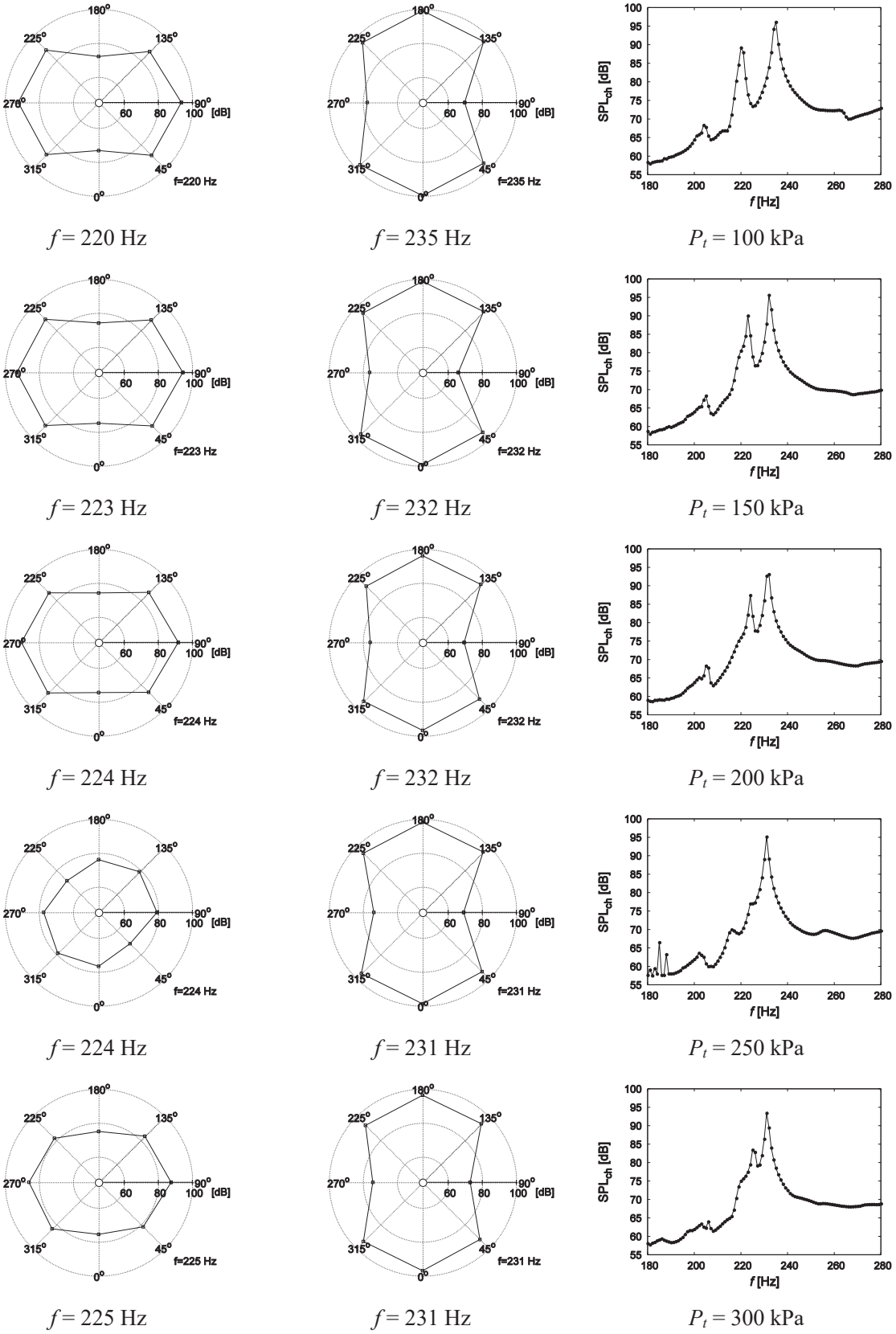

f = 220 Hz | f = 235 Hz | P_t = 100 kPa

f = 223 Hz | f = 232 Hz | P_t = 150 kPa

f = 224 Hz | f = 232 Hz | P_t = 200 kPa

f = 224 Hz | f = 231 Hz | P_t = 250 kPa

f = 225 Hz | f = 231 Hz | P_t = 300 kPa

Figure 5 Horizontal and vertical modes and channel average sound pressure level at each tire pressure

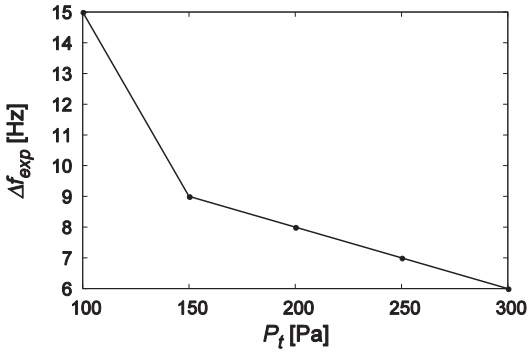

(a) Difference between horizontal and vertical mode frequencies with respect to tire pressure

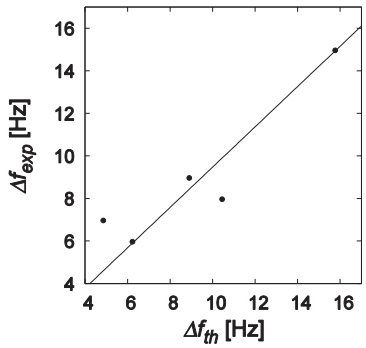

(b) Correlation of the difference between experimental and theoretical data (cross correlation coefficient = 0.94)

Figure 6 Difference between horizontal and vertical mode frequencies

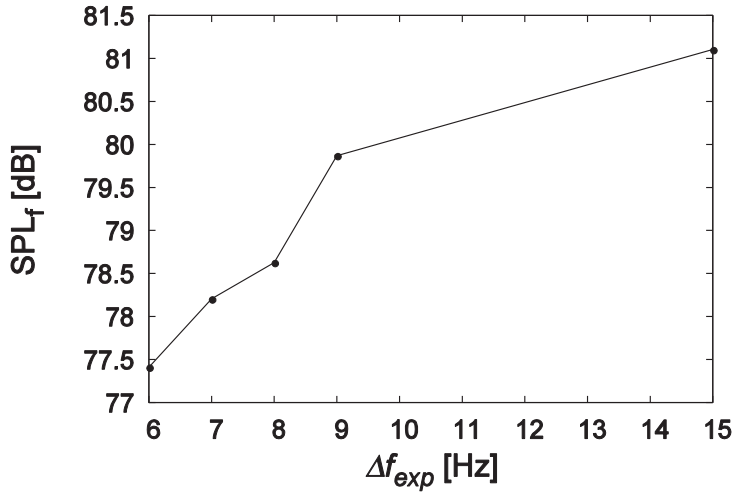

Figure 7 Frequency average sound pressure level with respect to difference between horizontal and vertical mode frequencies

5. CONCLUSIONS

We investigated the influence of the tire deformation on sound pressure level inside a tire around cavity resonance frequency. As a result, the sound pressure level will increase over a wide frequency range when the difference between horizontal and vertical mode frequencies becomes larger. The difference is theoretically determined by two parameters: length of the contact patch, and the ratio of the undeformed cross-sectional area to the deformed cross-sectional area in the contact patch. This difference is the primary source of the sound pressure level inside a deformed tire around the first tire cavity resonance.

REFERENCES

1. Heckl, M. Tyre noise generation. Wear 1986; p. 157-170.
2. Kropp, W. Structure-borne sound on a smooth tyre. Applied Acoustics. 1989;26(3):181-192.
3. Sakata, T., Morimura, H., Ide, H. Effects of tire cavity resonance on vehicle road noise. Tire Science and Technology. 1990;18(2):68-79.
4. Richards, T. L. Finite element analysis of structural-acoustic coupling in tyres. Journal of sound and

vibration. 1991;149(2):235-243.
5. Kim, G. J., Holland, K. R., Lalor, N. Identification of the airborne component of tyre-induced vehicle interior noise. Applied Acoustics. 1997;51(2):141-156.
6. Thompson, J. K. Plane wave resonance in the tire air cavity as a vehicle interior noise source. Tire Science and Technology. 1995;23(1):2-10.
7. Yamauchi, H., Akiyoshi, Y. Theoretical analysis of tire acoustic cavity noise and proposal of improvement technique. JSAE review. 2002;23(1):89-94.
8. Horikawa, S., Tanaka, Y., Murata, S., Theoretical analysis of tire acoustic cavity noise and proposal of improvement technique. Advanced experimental method. 2016;1 (to be published).
9. Gunda, R., Gau, S., Dohrmann, C., Analytical model of tire cavity resonance and coupled tire/cavity modal model. Tire Science and Technology. 2000;28(1):33-49.
10. Tanaka, Y., Horikawa, S., Murata, S. An evaluation method for measuring SPL and mode shape of tire cavity resonance by using multi-microphone system. Applied Acoustics. 2016;105:171-178.